International Journal of
Science and Engineering Investigations vol. 1, issue 9, October 2012
ISSN: 2251-8843

# Effect of Inclination of Impinging Jets on Flow and Heat Transfer Characteristics

Mizuki Kito
Department of Mechanical Engineering, Suzuka National College of Technology, Japan
(kito@mech.suzuka-ct.ac.jp)

***Abstract*-**The present study deals with the flow and heat transfer characteristics of inclined, as opposed to perpendicular or normal, impinging jets. Extensive visualization experiments are conducted and a digital camera analyzed the flow. In order to further understand the effect of the inclination of impinging jets, the heat transfer distributions along a target plate are also measured. From the results taken, Nusselt number is calculated and compared to the case of inclined single impinging jets. Furthermore, a comparison between a single jet and twin-jet inclined to face each other was made, and how the heat transfer characteristics are affected by the jet inclination is presented. The heat transfer experiments are conducted under Reynolds number $5.0 \times 10^3$, and the normalized nozzle-to-plate spacing $H/D_h$ (H: nozzle-to-plate spacing, $D_h$: the hydraulic diameter of the slot nozzle) ranging from 3 to 7, and the jet inclination ranging from $\theta$=0~60°, giving valuable information regarding the changes that occur due to the inclined impinging jets.

***Keywords-*** *Heat transfer; Inclined twin jet; Jet cooling.*

## I. INTRODUCTION

Impinging jets are used in a wide variety of applications to dry off wet surfaces or especially, to cool heated objects because of their high heat and mass-transfer characteristics in the stagnation region. Therefore, many researchers have investigated the effects of nozzle configuration including non-circular nozzles to improve the heat transfer rate on the target plate and the mechanism of the turbulent heat transfer [1, 2, 3]. Viskanta [4] provided detailed reviews of impingement heat transfer. Since the understanding of free jets is essential to reveal the mechanism of impinging jets and improve technical methods, the effects of nozzle configurations, jet velocity, and ambient conditions have been well addressed. Single impinging jets have been especially well studied, and it is well known that the heat transfer characteristics improve when jets impinge at the potential core length because of their high turbulence intensities and adequate velocity. However, while high heat transfer can be obtained at the stagnation region, the heat transfer rapidly decreases in the downstream.

Some researchers have reported the improvement of cooling efficiency and the heat transfer in the downstream using multi-impinging jets and turbulence promoters. Still, the majority of investigators have dealt with single impinging jets which impinge on a plate perpendicularly, not inclined mult-impinging jets. Regarding inclined impinging jets, Beitelmal et al. [5] studied the effects of inclination for a single rectangular jet, and Abdel-Fattah [6] demonstrated the flow structures for twin jets which are obliquely arranged. However, a problem seems to lie in the fact that the high heat transfer coefficient of a jet decays rapidly with the increase of distance downstream of the stagnation point. In this paper, we present the heat transfer characteristics of inclined-jet and inclined twin-jet impingement.

The experiments were divided into two parts. The first experiment was conducted with a single jet to demonstrate the effects of the inclination. The normalized nozzle−wall distance was kept constant at $H/D_h$ =2.0. The jet inclination was changed from 0 to 60 and the normalized nozzle-to-nozzle spacing was changed from 3 to 7. The second experiment presented flow and heat transfer measurement of twin-jet impingement. Both experiments were conducted at Reynolds number $Re$=5.0×10$^3$ based on the nozzle exit width $B$=5.0 mm and the jet exit velocity.

## II. NOMENCLATURE

| | |
|---|---|
| $A$ | Target plate area [m$^2$] |
| $B$ | Nozzle width (=5.0 mm) |
| $D_h$ | Hydraulic diameter of nozzle exit [m] |
| $H$ | Nozzle – plate distance [m] |
| $h$ | Heat transfer coefficient [W/m$^2$ K] |
| $L$ | Nozzle-to-nozzle spacing [m] |
| $Nu$ | Local Nusselt number (= $h D_h / \lambda_a$) |
| $\overline{Nu}$ | Average Nusselt number |
| $Pr$ | Prandtl number |
| $Q$ | Net heat flux [W/m$^2$] |
| $Re$ | Reynolds number (= $u D_h / \nu$) |
| $T$ | Temperature [K] |
| $T_a$ | Ambient temperature [K] |
| $u$ | Mean velocity [m/s] |
| $u_{max}$ | Maximum velocity [m/s] |
| $x$ | Coordinate in stream direction |
| $\theta$ | Jet angle [degree] |
| $\rho$ | Air density [kg/m$^3$] |

$\nu$ Coefficient of kinetic viscosity [ $m^2/s$ ]

$\lambda_a$ Air thermal conductivity [W/m K]

## III. EXPERIMENTAL PROCEDURE

The entire experimental set-up is sketched in Fig. 1. After the flow rate and air temperature were controlled by the valve and the air, the air ejects from the nozzle into ambient air with a temperature that was kept constant with the jet temperature within ± 0.1 ºC during the measurements.The target plate was made of Bakelite and was 20 mm thick. Direct heating of a thin (40-μm) stainless steel foil attached to the plate done electrically with a uniform heat flux adjusted by a slide trance. The net heat amount was calculated considering the heat transfer rate to the plate and the thermal radiation from the foil surface. The conduction and thermal radiation heat transfer were approximately 3% during a typical experiment. A total of 38 thermocouples (C-A) were placed 4 mm apart on the back side of the foil to measure the temperature distributions on the plate simultaneously by a data logger within 0.1°C accuracy.

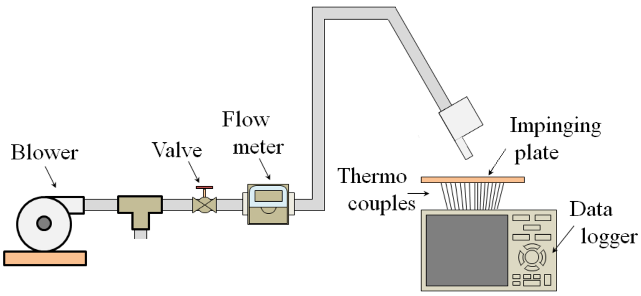


Figure 1. Experimental apparatus

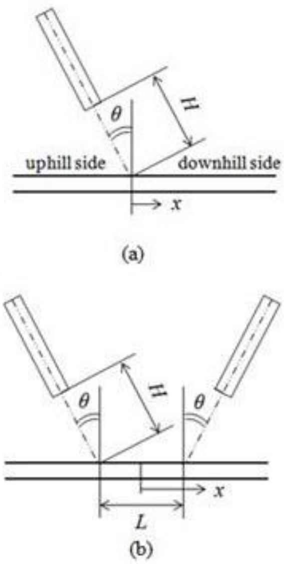


Figure 2. Coodinate systems for single and inclined twin impinging jets

The flow rate of the jet and the air temperature were controlled by a valve and cooler. During the experiment the air issued from the nozzle to the plate. The nozzle used in this experiment had a rectangular exit area 5 mm × 50 mm, giving it an aspect ratio of 10. The normalized nozzle-plate distance was kept at $H/D_h$=2 where $D_h$ is the hydrical diameter, and the Reynolds number $Re$=5.0×$10^3$ was a constant, while the nozzle angle was changed from 0 to 60 degrees. We conducted two experiments; a single inclined impinging jet, twin impinging jets inclined to face each other as shown in Fig.2 (b). The effects of jet spacing $L$ on the heat transfer were also investigated. As shown in Fig.2 (a) the direction toward which the nozzle inclined is defined as the "uphill side" and the other direction is defined as the "downhill side". The coordinate system takes $x$ starting from the center of the plate to the downhill side.

In order to investigate the nozzle properties, the free jet centerline velocity was measured without the target plate. The normalized centerline velocities $u/u_{max}$ ($u_{max}$ is the maximum or initial velocity at the nozzle exit) of the nozzle are shown in Fig. 3. The centerline velocity remained almost constant from the nozzle exit up to $x/D_h$ =1.7 where $D_h$ is the hydraulic diameter. When the potential core length is taken as the distance from the nozzle exit where the jet velocity decays to 95% of its maximum, the potential core existed up to approximately $x/D_h$= 2.5. Thereafter, the velocity decayed with $u/u_{max} \propto (x/D_h)^{-0.5}$ in the fully developed region, which is the empirical equation in the fully developed region for a rectangular nozzle. It is clear that the centerline velocity profile is remarkably well fitted by the distinctive equation, which confirms the reliability of the nozzle used in the presented experiment.

The local heat transfer coefficient was calculated from the temperature distribution along the $x$ axis using the thermocouples on the back side of the plate and the jet flow temperature as shown in (1).

$$h = \frac{Q}{A(T - T_a)} \tag{1}$$

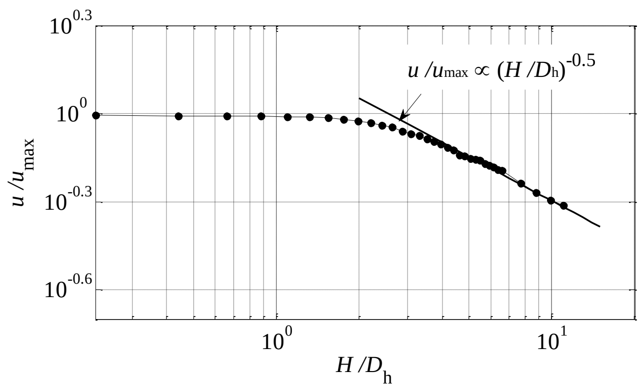


Figure 3. The centerline velocity

where $A$ is the smooth target plate area, $T$ is the impingement wall temperature measured by the thermocouples, and $T_a$ is the room temperature. In the estimation of the net heat flux $Q$, the heat loss due to thermal conduction into the target plate $Q_c$ and thermal radiation from the surface $Q_r$ were considered and calculated by (2). The heat loss due to thermal conduction was estimated by the difference of the plate inner temperature and the impinging plate surface temperature.

$$Q = Q_{input} - Q_c - Q_r \tag{2}$$

The mean heat transfer coefficient $\bar{h}$ was defined as shown in (3).

$$\bar{h} = \frac{1}{A}\int h(x)dx \tag{3}$$

where $x$ is the distance from the stagnation point.

The local Nusselt number was defined as follows:

$$Nu = \frac{h \cdot d}{\lambda} = \frac{Q \cdot D_h}{\lambda_a \cdot A(T - T_\infty)}, \tag{4}$$

where $\lambda_a$ is the air thermal conductivity and the characteristic length is the hydraulic diameter.

H. Martin [7] defined the entrainment factor as the temperature ratio between the jet-ambient and the jet-impinging plate surface, the value of which affects the heat transfer reduction. The jet temperature in all cases was controlled carefully to keep constant within $\pm 0.1^\circ C$ of the atmospheric temperature. Thus, the effect of entrainment claimed by H. Martin [7] could be neglected.

Before investigating the effects of jet inclination on the heat transfer characteristics, a validity check was conducted. Fig. 4 demonstrates the heat transfer at $Re_B$=10×10$^3$, $H/B$=10. The stagnation $Nu$ when a rectangular nozzle jet impinges was evaluated in [8] as follows.

$$Nu_B = 1.42 \cdot Pr^{0.43} \cdot Re_B^{0.58} \cdot (H/B)^{-0.02}$$
$$\left(10^4 < Re_B < 10^5\right) \tag{5}$$

where $Re_B$ is the Reynolds number based on the nozzle width. The stagnation $Nu$ was 65.3 in Fig. 4 and $Nu_B$=61.3 was obtained from (5). Good agreement of about 6.7% was achieved for the impingement cooling characteristics.

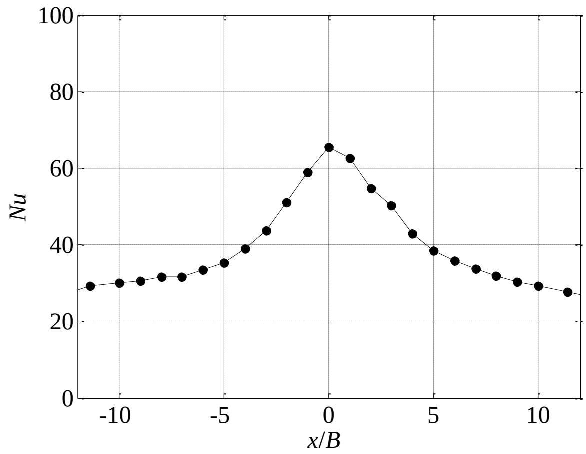


Figure 4. Local Nusselt number for single impinging jet at Re=10×10$^3$, H/B=10

## IV. RESULTS

### A. Single inclined impinging jet

Maximum heat transfer occurs at the stagnation point and the local $Nu$ decreases gradually in the downstream when a single jet impinges on the plate in a direction normal to the plane ($\theta$ = 0°). Fig.5 shows the local $Nu$ distributions for various nozzle angles. The local $Nu$ in the uphill side rapidly decreases, while that in the downhill side gradually increases. Therefore, uniform cooling on the downhill side was successfully achieved.

Fig.6 depicts the magnified figure of Fig.5 to demonstrate the location of the maximum $Nu$ of single impinging jets when the nozzle angle $\theta$ is changed from 0 to 60 degrees. The maximum $Nu$ shifts to the uphill side from the geometrical stagnation point and its value decreases as the angle increases. It is worth noting that the shift value increases and reaches its maximum at 45 degrees. At $\theta$ > 45°, the maximum $Nu$ shifts back to the downhill side.

The vortex structures of the impinging jets were visualized by the tracer method and the flow visualization was performed. Air jets seeded homogenously using a W-515 fog machine (ANTARI) issued from the nozzle into the still fluid. The images of vortex structures were recorded with a digital video camera by illuminating the flow in the middle plane using a xenon light sheet. The flow visualization was conducted in a dark room to maintain the same conditions throughout the experiments. Fig. 7 presents a selected sample of the visualized flow patterns in the middle plane of the inclined jet at $\theta$ = 45° and large vortex structure can be clearly seen. The location where the large vortex rolling-up which is indicated by the arrow, occurs is consistent with the maximum heat transfer. It is, therefore, considered that the large vortex rolling-up causes the maximum $Nu$ shifts to the uphill side at $\theta$ < 45°. However, at $\theta$ > 45°, the momentum of the wall jet flow to the downhill side becomes large, which causes that the maximum $Nu$ shifts back to the downhill side.

Fig. 8 shows the variation of average $Nu$ over the plate (-12 < $x/D_h$ < 12) and in the downstream (-12 < $x/D_h$ < -6; 6 < $x/D_h$ < 12). The increasing rate of the average $Nu$ compared with the normal impinging jet is also presented in Fig. 9. The average $Nu$ over the plate decreases as $\theta$ increases; however, the maximum values of $Nu$ at $\theta$ < 30° are as high as that of the normal jet. The average $Nu$ over the plate rapidly decreases at

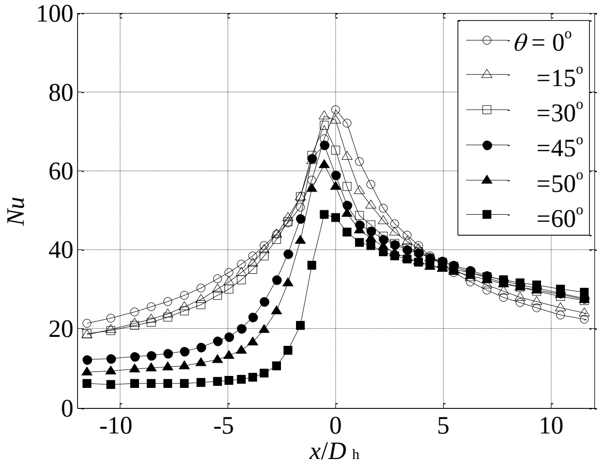


Figure 5. Local Nusselt number for single inclined impinging jet

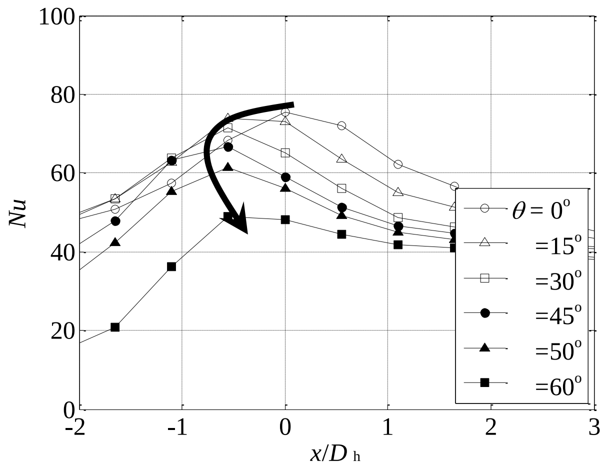


Figure 6. Local Nusselt number for single inclined impinging jet

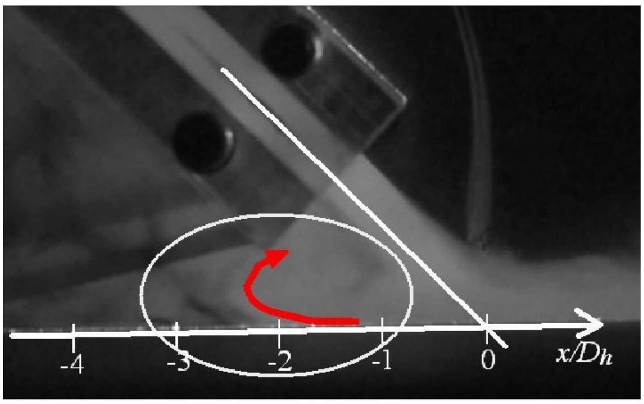


Figure 7. Flow visualisation ($\theta$=45°)

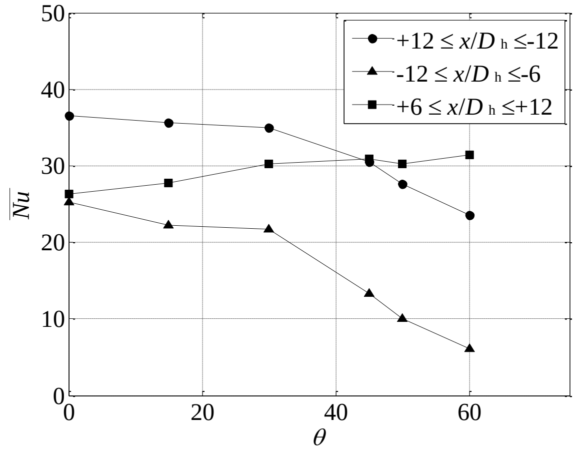


Figure 8. Variation of average Nusselt number

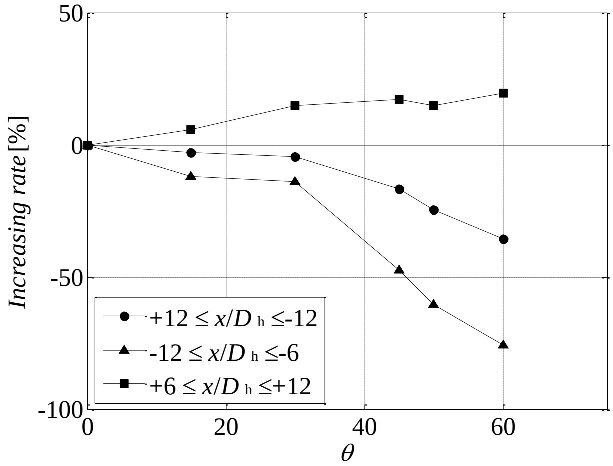


Figure 9. Increasing rate of the average Nusselt number compared with normal impinging jet

$\theta > 30°$. This explains that the small inclination of a jet $\theta < 30°$ hardly affects the heat transfer characteristics over the plate, while inclinations of $\theta > 30°$ cause significant decrease in the heat transfer. The average *Nu* in the uphill side decreases as θ increases. Especially, at $\theta > 30°$ the average *Nu* in the uphill side decreases significantly. On the contrary, the average *Nu* in the downhill side increases as $\theta$ increases. The average *Nu* increased a maximum of 19% in the downhill side compared with the normal jet. Since a flat average *Nu* can be obtained in the downhill side, an inclined impinging jet can uniformly cool a heated plate in the downstream.

### *B. Twin impingeing jets*

Fig. 10 shows the local *Nu* when the jet spacing was changed from $L/D_h$ = 3 to 7. In the case of $\theta$ = 0°, two peaks appear at the same location as the geometric stagnation point. The peak value appeared to be independent of the stagnation distance and increased about 2% higher than that of the single jet. The average *Nu* over the plate was enhanced by about 20%

compared to the single jet; naturally, twin jets can improve the heat transfer on the impingement plate.

A second peak appears at the center of the plate when the jet spacing is wide enough to produce rolling-up effects. However, a comparison of the second peaks at $L/D_h$=5 and 7 clearly indicates that the second peak at $L/D_h$=5 is higher than that at $L/D_h$=7. This is attributed to the momentum loss decaying the impinging velocities of wall jets as the jet spacing increases. A higher second peak occurs when the jet spacing is smaller; however, when the jet spacing is too small, a second peak cannot be seen.

Fig.11 shows increasing rate of the average *Nu* of normal twin impinging jets over the plate compared with the normal single jet. The average *Nu* at both $L/D_h$=3 and 7 increases over 20 %, which indicates that the second peak at the center of the jets increases when the rolling-up occurs and that interference between two impinging jets less affect the decrease in the heat transfer at the center of the jets when the jet spacing is small.

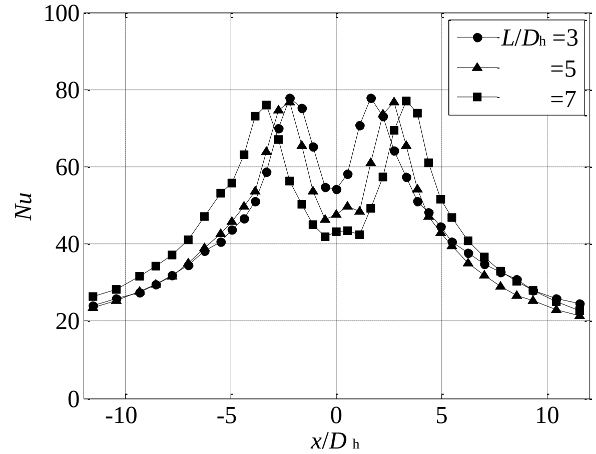


Figure 10. Local Nusselt number for twin impinging jets ($\theta$=0°)

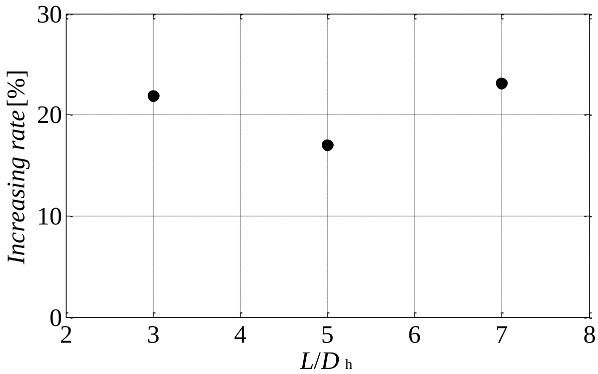


Figure 11. Increasing rate of the average Nusselt number over the plate compared
with the normal single jet

### C. Twin impingeing jets inclined to face each other

Figs. 12 and 13 show the local *Nu* when the twin impinging jets are inclined to face each other as shown in Fig.2 (b). Each distribution in Figs. 12 and 13 indicates the second *Nu* peak at the center of the jets since the wall jet flowing from each nozzle impinges at the center, producing high turbulence intensity which contributes to breaking the thermal boundary layer along the plate. The second *Nu* peak becomes smaller as the jet spacing increases because the wall jet flows lose kinetic energy at the time of impingement.

The twin-jet flow visualization by illuminating the flow in the middle plane using a xenon light sheet is shown in Fig.14. At the center of the jets where the second *Nu* peak was observed in the heat transfer measurements, the wall jets interference produces a rolling-up or an upwash motion. The rolling-up motion promotes the heat transfer.

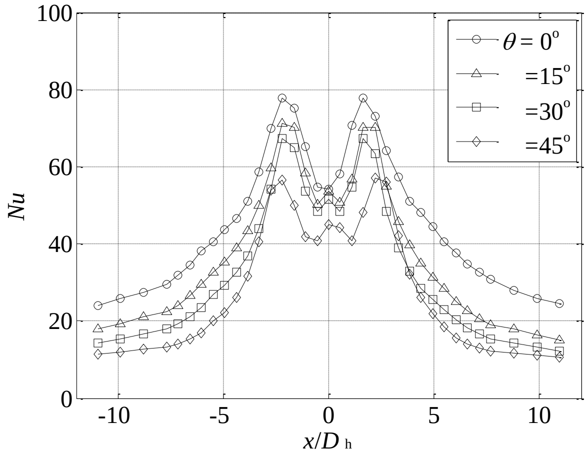


Figure 12. Local Nusselt number for inclined twin impinging jets ($L/D_h$=3) inclined to face each other

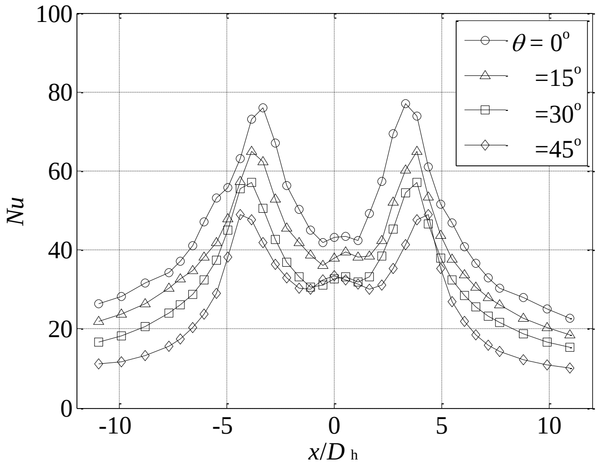


Figure 13. Local Nusselt number for inclined twin impinging jets ($L/D_h$=7) inclined to face each other

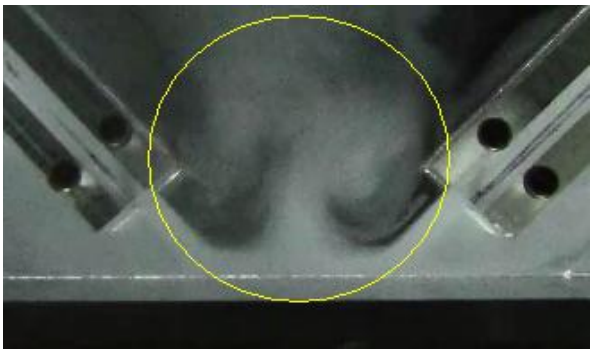

Figure 14. Flow visualisation ($L/D_h$ = 3, $\theta$=45°)

## V. CONCLUSION

The effects of inclination angle of impinging jets on cooling characteristics were investigated. We conducted two experiments: a single inclined impinging jet and twin impinging jets inclined to face each other. The main results obtained were:

1) In the case of a single inclined jet, the local *Nu* increases in the downhill side as $\theta$ increases, while the *Nu* in the uphill side decreases. The average *Nu* ($-12 < x/D_h < 12$) improved up to 19% compared with that of $\theta = 0°$. The maximum *Nu* decreases as $\theta$ increases and the *N*u peak position shifts towards the uphill side until $\theta$ = 45° and shifts back at $\theta \leq 45°$.

2) In the case of normal twin jets, the first *Nu* peak appeared at the same position as the geometrical stagnation point. The first *Nu* peaks were little affected by jet spacing. The second *Nu* peak appeared at the center of the jet impingement points. The *Nu* peak was strongly affected by jet spacing. The average *Nu* improved about 20% compared with that of a single jet.

## REFERENCES


[1] Lee, J. & Lee, SJ., The effect of nozzle configuration on stagnation region heat transfer enhancement of axisymmetric jet impingement. *Int. J. Heat and Mass Transfer*, **43 (18)**, pp. 3497-3509, 2000.

[2] Kataoka, K., Suguro, M., Degawa, H., Maruo, K. & Mihata, I., Effect of Surface Renewal Due to Large-Scale Eddies on Jet Impingement Heat Transfer. *Int. J. Heat and Mass Transfer*, **30**, pp. 559-567, 1987.

[3] Yokobori, S., Kasagi, N., Hirata, M. & Nishiwaki, N., Role of Large-Scale Eddy Structure on Enhancement of Heat Transfer in Stagnation Region of Two-Dimensional, Submerged, Impinging Jet. *Proc. of the 6th Int. Heat Transfer Conf.*, Canada, pp. 305-310, 1978.

[4] R. Viskanta, Heat transfer to impinging isothermal gas and flame jets. *Exp. Thermal and Fluid Science*, **6**, pp. 111-134, 1993.

[5] Beitelmal, A.H., Saad, MA. & Patel, C.D., The effect of inclination on the heat transfer between a flat surface and an impinging two-dimensional air jet. *Int. J. Heat and Fluid Flow*, **21**, pp.156-163, 2000.

[6] Abdel-Fattah, A., Numerical and experimental study of turbulent impinging twin-jet flow. *Exp. Thermal and Fluid Sci.*, **31**, pp.1061-1072, 2007.

[7] H. Martin, “Heat and mass transfer between impinging gas jets and solid surface,” Adv. Heat Transfer, vol.13, 1977, pp.1-60.

[8] JSME Data Book; Heat Transfer 5th Edition, pp.39-51, 2009